# Cracking catalysts

**Document status and date:**
Published: 01/01/1980

**Document Version:**
Publisher's PDF, also known as Version of Record (includes final page, issue and volume numbers)

**Please check the document version of this publication:**

• A submitted manuscript is the version of the article upon submission and before peer-review. There can be important differences between the submitted version and the official published version of record. People interested in the research are advised to contact the author for the final version of the publication, or visit the DOI to the publisher's website.
• The final author version and the galley proof are versions of the publication after peer review.
• The final published version features the final layout of the paper including the volume, issue and page numbers.

[Link to publication](#)

Download date: 16. Nov. 2023

# CRACKING CATALYSTS

J.H.C. van Hooff

Laboratory for Inorganic Chemistry, Eindhoven
University of Technology, Eindhoven, The Netherlands

## INTRODUCTION

As mentioned before catalytic cracking reactions proceed via carbenium ion intermediates. A cracking catalyst has the function to assist in the formation of such carbenium ions from the feedstock molecules. Normally this can be done by acids, but in this special case the acid catalyst must have two special properties:

i.  It must be possible to use the catalyst in a fluid bed process, and

ii. The catalyst must be stable at temperatures up to $700^0 C$. Therefore the common acids like $H_2SO_4$, $HNO_3$, $H_3PO_4$ and HCl cannot be used.

Instead of these acids the so-called 'solid acids' have been developed. At first acid-treated clay minerals were used for this purpose but with little success. The development of the amorphous silica-alumina catalysts meant a big step forwards. However, the most important advance in catalytic cracking in the last three decades has been the development of zeolite catalysts. It is the purpose of this chapter to summarize the structures of cracking catalysts and their influence on cracking reactions.

## AMORPHOUS SILICA ALUMINA CATALYSTS

Neither $SiO_2$ (silica) nor $Al_2O_3$ (alumina) nor a mechanical mixture of the two dry oxides has acid properties, but a cogelled mixture of silica and 10 to 25% alumina can be used as an active cracking catalyst. The incorporation of alumina into silica results in the formation of surface acid sites which catalyze

cracking reactions.
The preparation of these so-called silica-alumina catalysts [1]
involves first the preparation of a porous silica hydrogel.
This hydrogel consists of a coherent aggregate of primary spherical
particles about 3 to 5 nm in diameter. The primary particles
consist of a three-dimensional network of interconnected $SiO_4$
tetrahedra, each silicon atom being linked to four oxygen atoms
and each oxygen atom linking two silicons. The surfaces of the
particles are terminated with hydroxyl groups in the form of
silanol (Si-OH) groups (see figure 1).



Figure 1 A primary particle of a silica
hydrogel with silanol groups at
the surface
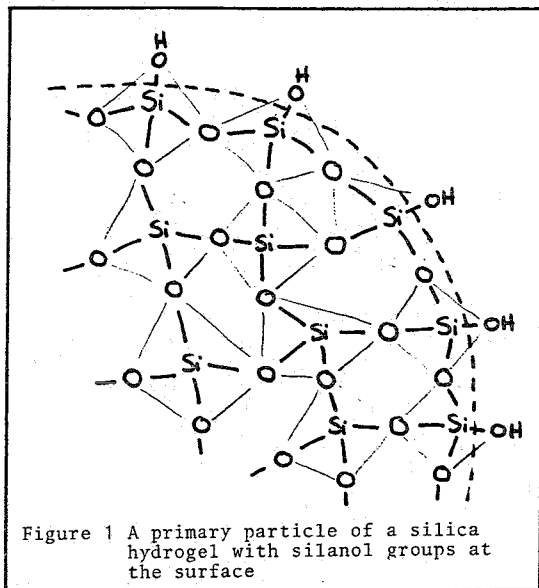
These silanol groups vary from weakly acidic to alcoholic and
show no cracking activity.

In the second step of the preparation an aluminum salt is
added to the silicahydrogel so that the six coordinated aluminum
ions react with the surface of the primary silica particles.
Reaction involves a condensation of the aluminum hydroxide with
the elimination of water. The result is that aluminum ions are
incorporated into the surfaces of the silica particles in the
form of $AlO_4$ tetrahedra (see figure 2).

Since the trivalent aluminum ion is bonded to four oxygen
anions each $AlO_4$ tetrahedron has a residual charge of -1.
Therefore each alumina tetrahedron requires a +1 charge from a
cation in the structure to maintain electrical neutrality.
If the condensation of the aluminum hydroxide is carried out at

Figure 2 Condensation reaction of aluminumhydroxide with the surface of a silica hydrogel
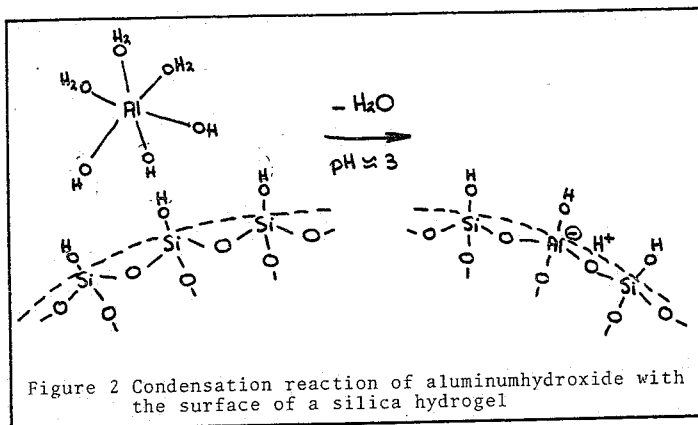
low pH (pH $\approx$ 3) H$^+$ ions will take this place.
This results in the formation of surface OH groups having strong Brønsted acid character.
The protonic acidity evidently arises from the dissociative adsorption of H$_2$O on the aluminum ion. It is associated with the proton which moves to the oxygen bonded to a neighbouring silicon ion (see figure 3).

Figure 3 Formation of proton acidity on silica-alumina
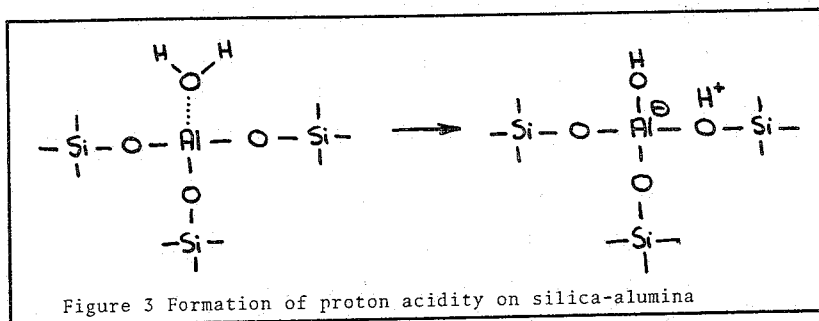
The strongly electrophilic nature of the aluminum ion can be traced to its position in the surface, where it is surrounded by 3 fourvalent silicon cations. This accounts for the withdrawal of charge from the aluminum ion to make it more positive and develop a sufficiently strong field to allow it to acquire a hydroxyl group by splitting off a proton from water. The resultant
$\qquad$ H
Si - O - Al group is strongly polarized, which induces a strong acidity in the group.

When the silica-alumina surface is heated to high temperature

(> about 400°C), water is removed from the Brønsted acid site,
exposing the aluminum ion with its electron-pair-acceptor
properties, thereby forming a Lewis acid site (see figure 4).



Figure 4 Conversion of a Brønsted acid site into a Lewis acid
         site by dehydration of silica alumina
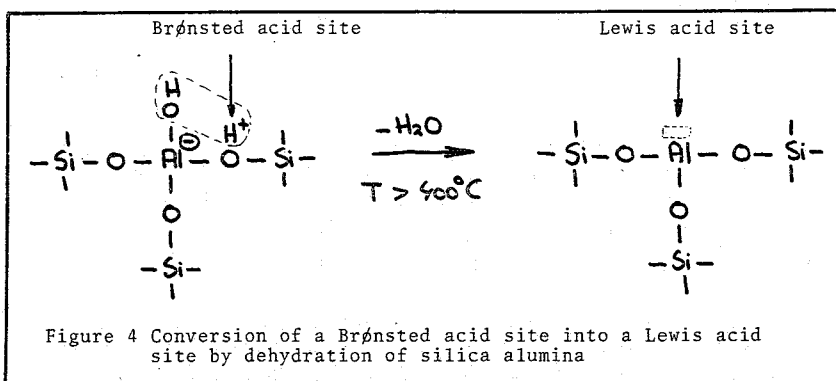
As the actual reaction temperature in the catalytic cracking
process is about 500°C especially the Lewis-acid sites of the
silica-alumina catalyst will play an important role.

Commercially two types of amorphous silica-alumina catalysts
are available:
Low Alumina (LA) with about 13% wt $Al_2O_3$ and
High Alumina (HA) with about 25% wt $Al_2O_3$

Typical analyses of fresh LA and HA catalysts are [2]

| Chemical composition | | LA | HA |
|---|---|---|---|
| Loss on ignition (1 hr 1000°C wt% wet base) | | 16 | 15 |
| $Al_2O_3$ | wt% dry base | 13 | 25 |
| $Na_2O$ | wt% dry base | 0,02 | 0,02 |
| $SO_4^-$ | wt% dry base | 0,2 | 0,7 |
| Fe | wt% dry base | 0,02 | 0,03 |
| $SiO_2$ | wt% dry base | balance | balance |

| Physical properties | | | |
|---|---|---|---|
| Surface Area (1 hr 600°C) | $m^2/g$ | 600 | 510 |
| Pore Volume ($H_2O$) | ml/g | 0,7-1,1 | 0,75 |
| Apparent Bulk Density | g/ml | 0,33-0,40 | 0,42 |
| Attrition 1 hr | wt% | 22 | 16 |
| Average Particle Size | μm | 65 | 60 |

The thermal stability of these catalysts is limited especially in
the presence of steam as is the case during stripping and
regeneration. This causes sintering of the catalyst particles by
which the pore volume and the surface area decrease.

An 'equilibrium' LA catalyst has the following physical
properties

| LA catalyst | fresh | equilibrium |
|---|---|---|
| Surface Area $m^2/g$ | 600 | 100 |
| Pore Volume ml/g | 0,9 | 0,45 |
| Average Pore Diameter nm * | 6 | 18 |
| Apparent Bulk Density g/ml | 0,35 | 0,70 |

$$* \quad \overline{PD}(nm) = \frac{4 \times PV(ml/g)}{SA(m^2/g)} \times 10^3$$

Catalytic Cracking of Mid Continent Gasoil with a LA catalyst
results in the following product distribution

Feed:                Mid Continent Gasoil
Catalyst:            Low-Alumina
WHSV:                $2.0 \ hr^{-1}$
Reactor Temperature: $500^0C$

Product distribution   Total conversion 75%

Gas $C_1-C_4$:      15%         paraffins   10%
Gasoline $C_5^+$:   45%         olefins     45%
Light Cycle Oil: 10%           naphthenes  10%
Coke:             5%           aromatics   35%

As can be seen in this table besides gasoline relatively large
amounts of 'gas' and 'coke' are formed, leaving much room for
improvement. An important improvement could be realised by the
introduction of cryatalline zeolite cracking catalysts.
A description of this type of catalysts will be given in the
next paragraph.


CRYSTALLINE ZEOLITE CATALYSTS

About twenty years ago coworkers of Mobil and Exxon [3, 4]
discovered that special molecular-sieve zeolites could be used
as effective cracking-catalysts.
Further development of this finding at which besides Mobil and
Exxon also Union Carbide has contributed, has resulted in improved
cracking catalyst with the following advantages with respect to
the amorphous silica-alumina catalysts

- higher activity
- higher gasoline selectivity
- higher stability.

To understand this behaviour we first have to explain the zeolite structure and the origin of its acidity.

Zeolites are crystalline alumino-silicates, with $SiO_4$ and $AlO_4$ tetrahedra as fundamental building blocks. These tetrahedra are arranged in such a way that each of the four oxygen anions is shared with another silica or alumina tetrahedron to form a threedimensional crystal lattice.

The zeolite that is most applicated in cracking catalysts (type X or Y) has a crystal-structure related to the mineral faujasite. In this structure 24 $SiO_4$ and/or $AlO_4$ tetrahedra form together a secondary building unit in the form of a cubo-octahedron the so-called sodalite-unit (see figure 5).



24 $SiO_4$ and/or $AlO_4$ tetrahedra

Figure 5 The structure of a cubo-octahedron or sodalite cage
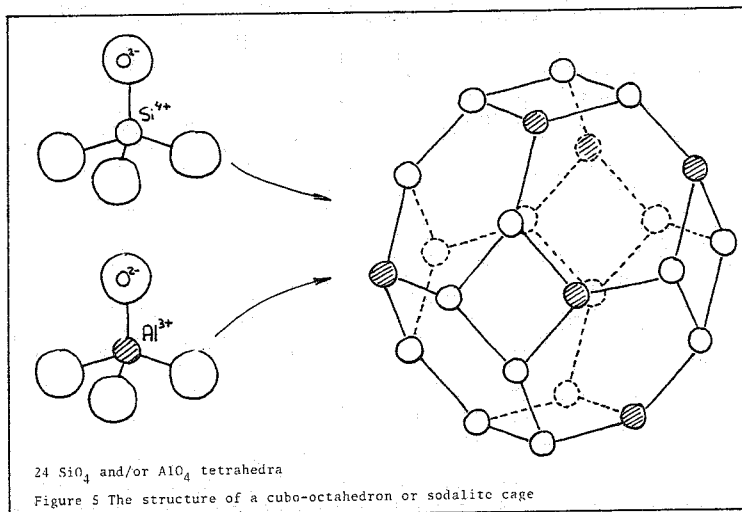
In the sodalite-unit we can distinguish 6 four-membered rings (the faces of a cube) and 8 six-membered rings (the faces of an octahedron)

Coupling of the cubo-octahedra to form crystalline structures can occur in different ways

i.   When the cubo-octahedra are stacked so that each four-membered ring is shared by two units, sodalite is formed (see figure 6).

ii.  When the cubo-octahedra are connected by bridge oxygen atoms between the four-membered rings, zeolite A is formed (see figure 7).

iii. The third possibility is that the cubo-octahedra are connected by bridge oxygen atoms between the six-membered rings. In that case the faujasite-type zeolite is formed (see figure 8)

Figure 6 The arrangement of the
cubo-octahedra in
sodalite



Figure 7 The arrangement of the cubo-octahedra
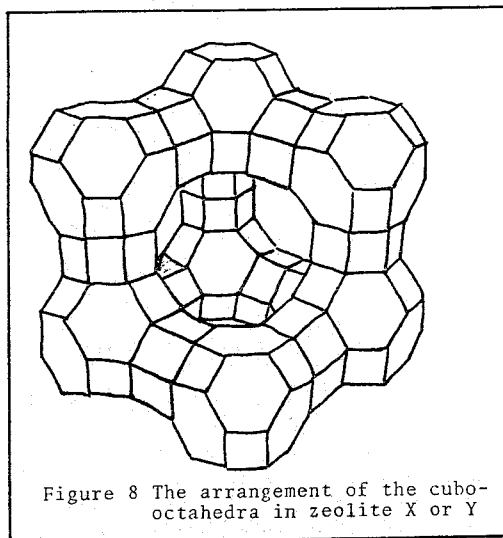in zeolite A
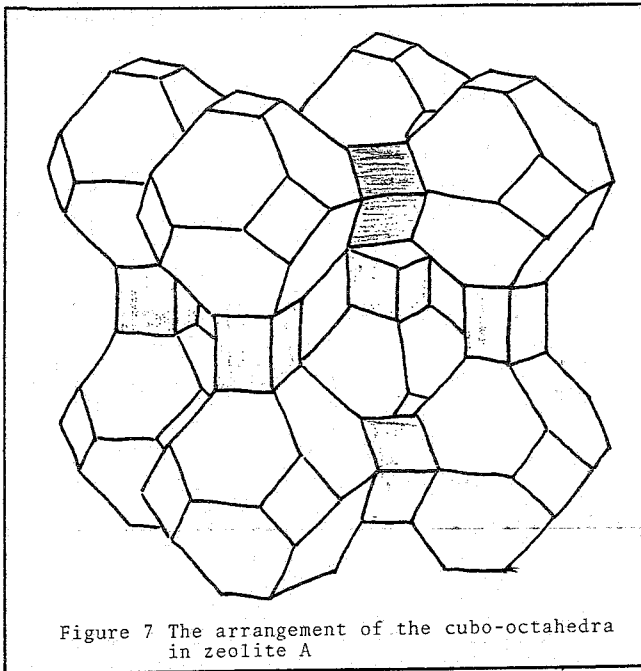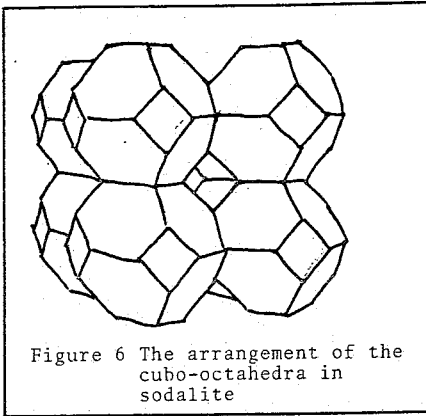
Figure 8 The arrangement of the cubo-
octahedra in zeolite X or Y

The synthetic forms of this type of zeolite generally are in-
dicated by type X-zeolite or type Y-zeolite depending on the
Si/Al ratio.

    type X zeolite          Si/Al = 1,0 - 1,5
    type Y zeolite          Si/Al = 1,5 - 3,0

As can be seen in the figures 6, 7 and 8 zeolite A and especially
zeolite X and Y have open structures with relatively large cavities
that are interconnected with windows of six-, eight- and twelve-
membered rings. In this way a highly porous framework is formed,
that allows molecules with dimensions up to the free aperture
of the window to enter the cavities.

    The characteristic dimensions of the pore systems in zeolite
A and zeolite X and Y are listed below [5].

|  | zeolite A | zeolite X and Y |
|---|---|---|
| Supercage or $\alpha$-cage |  |  |
| free diameter $A^o$ | 11.4 | 12 |
| aperture $A^o$ | 4,2 | 7.4 |
| Sodalite cage or $\beta$-cage |  |  |
| free diameter $A^o$ | 6.6 | 6.6 |
| aperture $A^o$ | 2.6 | 2.6 |
| Hexagonal prism or $\gamma$-cage |  |  |
| aperture $A^o$ | – | 2.6 |
| density g/ml | 1.33 | 1.30 |
| void volume ml/g | 0.30 | 0.35 (51%) |

As was the case in the amorphous silica-alumina catalysts the
presence of a $Al^{3+}$ ion in a $AlO_4$ tetrahedron creates an effective
negative charge. This charge is partially delocalized over the
entire structure, but the extent of the delocalization is not
known. The excess of negative charge is neutralized by positive
ions that are located on special positions in the zeolite structure.
In the X and Y zeolites, four distinct cation sites have been
located as shown in figure 9 [6].



Figure 9 Cross-sectional view of sodalite unit
and two adjoining hexagonal prisms indicating
the positions of the distinct cation sites
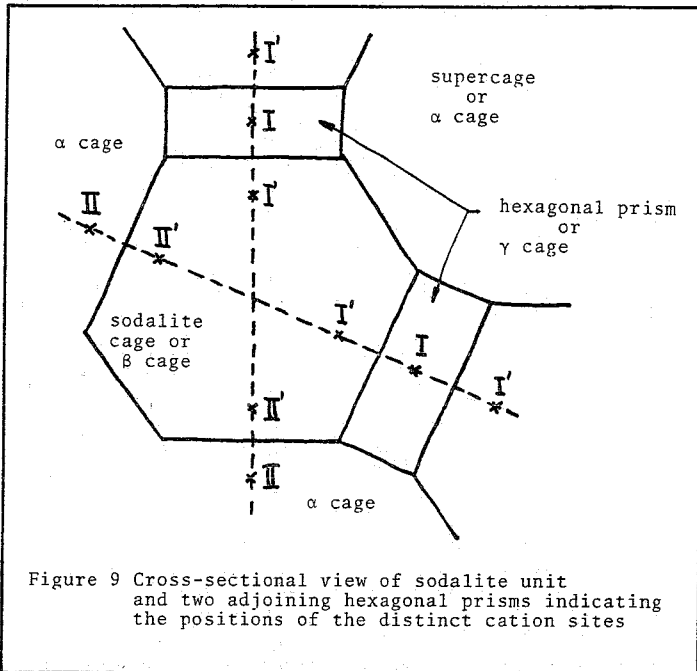
The type I site is located at the center of the hexagonal prism
formed by the six bridging oxygens; there are 16 type I sites per
unit cell.
The type I' site is located in the sodalite-unit just on the other
side of the shared hexagonal face from the type I site; there are
32 type I' sites per unit cell.
Type II and II' sites are located on the unjoined hexagonal
faces of the sodalite units respectively outside and inside the
sodalite cage; there are 32 of each of these sites per unit cell
Therefore the total number of cation site is 16 + 32 + 32 + 32 = 112.
This number exceeds the number of cations that are really present
in zeolite X or Y so that the sites are only partly occupied.

    This can be illustrated by the following example:
let us start from a Y zeolite with a Si/Al ratio of 2.5.
Per unit cell we have 8 cubo-octahedra and thus 8 x 24 = 192
$SiO_4$ and/or $AlO_4$ tetrahedra. Because Si/Al = 2.5 these 192

tetrahedra can be devided in $\frac{2.5}{3.5}$ x 192 = 136 $SiO_4$ tetrahedra and

$\frac{1.0}{3.5}$ x 192 = 56 $AlO_4$ tetrahedra.

For every $AlO_4$ unit we need a +1 charge in the form of a cation; thus totally a cation charge of +56 is needed.
As Y zeolites are synthesized in the presence of $Na^+$ ions, 56 of these $Na^+$ ions will be incorporated in a unit cell divided over the 112 available cation sites. Furthermore up to about 260 water molecules can be absorbed per unit cell. This results in the following unit cell formula for the sodium-form of zeolite Y also indicated by NaY (see figure 10).

$$Na_{56} \left[ (AlO_2)_{56} \; (SiO_2)_{136} \right] \; 260 \; H_2O$$

$$\underbrace{\phantom{Na_{56}}}_{\substack{\text{cations for} \\ \text{charge equilibrium}}} \quad \underbrace{\phantom{(AlO_2)_{56} (SiO_2)_{136}}}_{\text{zeolite skelet}} \quad \underbrace{\phantom{260 H_2O}}_{\text{adsorbed water}}$$
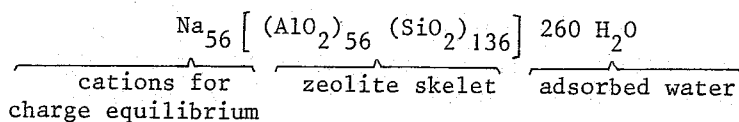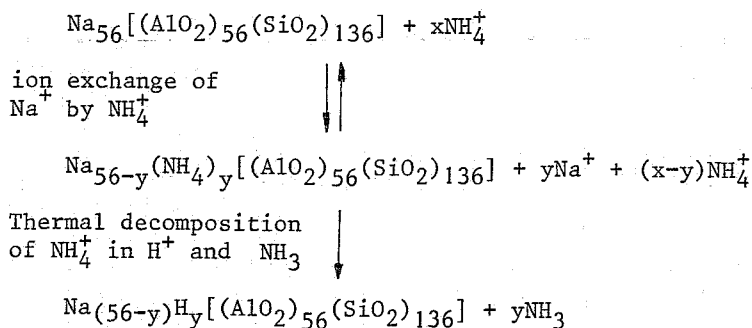
Figure 10    Unit-cell formula of NaY

In this form the zeolite shows almost no catalytic activity. This activity is developed if acid groups are introduced in the zeolite. For this purpose we can use the cation-exchange properties of the zeolite. The $Na^+$ cations present in the zeolite skelet can be exchanged by other cations by a standard ion-exchange procedure. Analogously to the amorphous silica-alumina we may expect that exchange of $Na^+$ against $H^+$ will result in the development of acidic groups. however, because of the poor stability of the Y zeolite in acid solutions the exchange of $Na^+$ by $H^+$ cannot be done by a simple treatment with diluted acids. We have to use a circuitous route.
One method is to exchange $Na^+$ by $NH_4^+$ first, followed by a thermal decomposition of the $NH_4^+$ ions in $H^+$ and $NH_3$.
The proceeding reactions can be expressed by the following reaction equations

$$Na_{56}[(AlO_2)_{56}(SiO_2)_{136}] + xNH_4^+$$

ion exchange of
$Na^+$ by $NH_4^+$             $\updownarrow$

$$Na_{56-y}(NH_4)_y[(AlO_2)_{56}(SiO_2)_{136}] + yNa^+ + (x-y)NH_4^+$$

Thermal decomposition
of $NH_4^+$ in $H^+$ and $NH_3$        $\downarrow$

$$Na_{(56-y)}H_y[(AlO_2)_{56}(SiO_2)_{136}] + yNH_3$$

A second method to illustrate this modification is shown in figure 11



Figure 11 Two-dimensional representation of the exchange
of $Na^+$ by $NH_4^+$, followed by a thermal decomposition
of $NH_4^+$ and $NH_3$
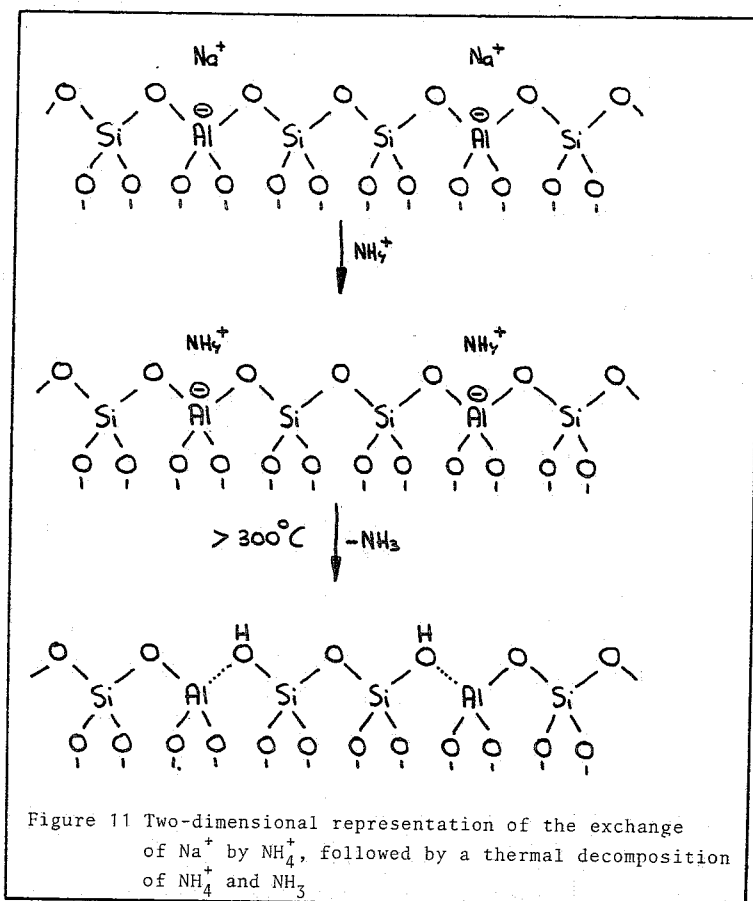
$\phantom{xxxxxxx}$ H
The Al – O – Si group obtained in this way possesses Brønsted
acidic properties as will be shown later on.
At temperatures above about $600^0C$ dehydroxylation occurs, resulting
in the transformation of the Brønsted-acid sites into Lewis-acid
sites (see figure 12).


At still increasing temperatures above about $750^0C$ the crystal
structure of the zeolite collapses resulting in an inactive
amorphous material

Figure 12 Transformation of Brønsted-acid sites into
Lewis-acid sites by heating above 500°C

A second method to introduce acidic properties is to exchange
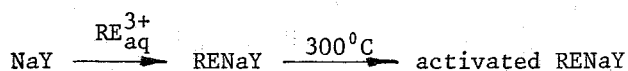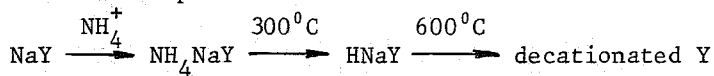the $Na^+$ ions against polyvalent cations ($Mg^{2+}$, $Ca^{2+}$ and by
preference $La^{3+}$)
Nowadays in commercial catalysts mostly threevalent rare-earth
ions are used.

> It is not necessary to use one of the pure rare-earth
> elements; the same results can be obtained if a mixture of
> rare-earth elements is used.
> Normally the natural mixture of the rare-earths with the
> following composition is used

| | | | | |
|---|---|---|---|---|
| La | about | 18% | Nd | about 24% |
| Ce | about | 46% | Sm | about 6% |
| Pr | about | 5% | others | traces |

The first step is the exchange of the $Na^+$ ions by the $RE^{3+}$ ions
by contacting the NaY zeolite with a aqueous solution of the
rare earth chlorides. Three $Na^+$ ions are replaced by one $RE^{3+}$
ion that under these circumstances will be hydrated.
The second step occurs by gently heating the exchanged zeolite.
At about 250°C one of the $H_2O$ molecules of the hydrate mantle
will be hydrolyzed under the influence of the threevalent rare-
earth ion. This is shown schematically in figure 13.

Figure 13 The development of Brønsted-acid site after exchange of Na$^+$ by La$^{3+}$ followed by acid hydrolysis

The Brønsted-acid-sites formed in this way are also transformed into Lewis-acid-sites by heating above 600$^0$C, as with the acid-zeolite obtained by NH$_4^+$ exchange.

However, the RE-exchanged zeolite has a better thermal stability than the NH$_4$-exchanged one. The collapse temperature can be increased up to 900$^0$C depending on the rest Na content of the zeolite.

In literature often the following nomenclature is used to indicate the distinct steps

$$NaY \xrightarrow{NH_4^+} NH_4NaY \xrightarrow{300^0C} HNaY \xrightarrow{600^0C} \text{decationated Y}$$

$$NaY \xrightarrow{RE_{aq}^{3+}} RENaY \xrightarrow{300^0C} \text{activated RENaY}$$

The presence of Brønsted-acid sites on the surface of cracking catalysts can be shown in different ways; two of these,
    - the indicator-method and
    - IR spectroscopy,
will be discussed shortly.


i. The indicator-method [7]

The acid-strength of a Brønsted-acid site BH at a solid surface is derived from its proton donating ability and can be expressed by the equilibrium constant of the reaction

$$\underline{BH} \rightleftharpoons \underline{B}^- + H^+$$
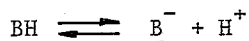
This equilibrium constant is given by:

$$K_{BH} = \frac{a_{H^+} \cdot a_{B^-}}{a_{BH}} = a_{H^+} \frac{f_{B^-} \cdot c_{B^-}}{f_{BH} \cdot c_{BH}} \tag{1}$$

so that:

$$pK_{BH} = -\log K_{BH} = -\log a_{H^+} \frac{f_{B^-} \cdot c_{B^-}}{f_{BH} \cdot c_{BH}} \tag{2}$$

Because in this case $a_{H^+}$ is not simple related to a concentration Hammett and Deyrup have introduced the 'acid-function' $h_o$ that is defined in the following way

$$h_o = a_{H^+} \frac{f_{B^-}}{f_{BH}} \tag{3}$$

or in logarithmic form

$$H_o = -\log h_o = -\log a_{H^+} \frac{f_{B^-}}{f_{BH}} \tag{4}$$

Combination of equations (2) and (4) than result in:

$$H_o = pK_{BH} + \log \frac{c_{B^-}}{c_{BH}}$$

The determination of this so-called Hammett function is based upon the reaction of the acid sites with a set of indicators with decreasing basic strength. In the table a number of these indicators are given together with the Hammett function of the acids that is needed for a colour change.

| Indicator | Basic colour | Acid colour | $H_o$ | $H_2SO_4$ conc wt% |
|---|---|---|---|---|
| Neutral red | yellow | red | +6.8 | $8 \times 10^{-8}$ |
| Phenylazonaphthylamine | yellow | red | +4.0 | $5 \times 10^{-5}$ |
| Butter yellow | yellow | red | +3.3 | $\times 10^{-4}$ |
| Benzeneazophenylamine | yellow | purple | +1.5 | 0.02 |
| Dicinnamalacetone | yellow | red | -3.0 | 48 |
| Benzalacetophenone | colourless | yellow | -5.6 | 71 |
| Anthraquinone | colourless | yellow | -8.2 | 90 |

The experimental method is as follows:
The zeolite from which the acid strength has to be determined is
suspended in benzene and a few drops of a non-aqueous solution
of one of the indicators is added. If a colour change is observed
it can be concluded that the zeolite contains acid-sites with an
acid-strength exceeding the Hammett function of the indicator used.
It can be shown in this way that RENaY contains acid-sites with
an acid-strength stronger than $H_o = -8.2$ (with anthraquinone a
colour change can be observed).
The quantity of these strong acid-sites can be determined by a
titration method as developed by Benesi. In this method increasing
amounts of n-butylamine are added before the addition of the
indicator.
From the amount of n-butylamine that is needed to obtain no colour
change of a certain indicator, the number of acid groups exceeding
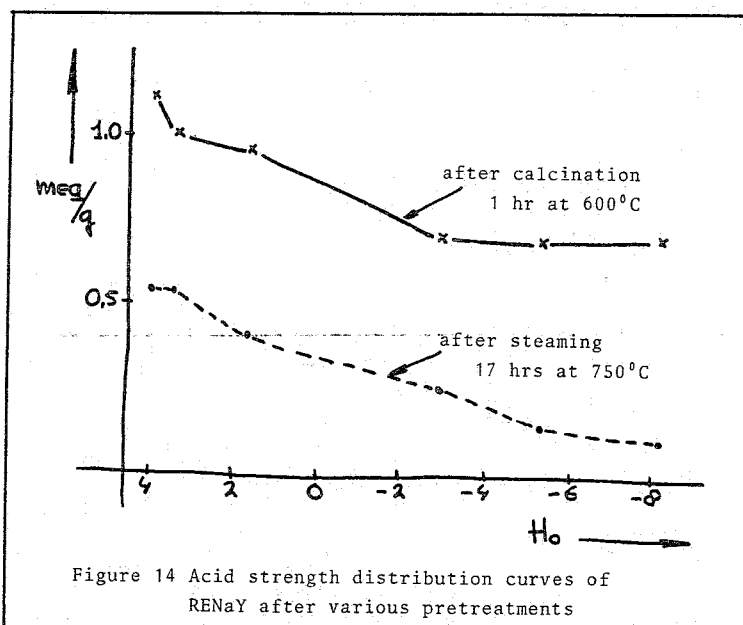the corresponding acid-strength can be determined.



Figure 14 Acid strength distribution curves of
RENaY after various pretreatments

By repeating this titration with the distinct indicators it is
possible to obtain an acid-strength distribution curve. For
RENaY the following distribution curve can be obtained [8]
(see figure 14).
It is shown in this figure that the acid-sites are influenced by
the pretreatment conditions. Hydrothermal treatment at $750^0C$
causes the disappearance of most of the very strong acid-sites
while the sites with medium acid-strength are only slightly
influenced.


ii. IR spectroscopy [9]

The IR spectrum of a HNaY zeolite obtained by heating $NH_4NaY$ at
$300^0C$ – $450^0C$ shows two characteristic absorption bands (see
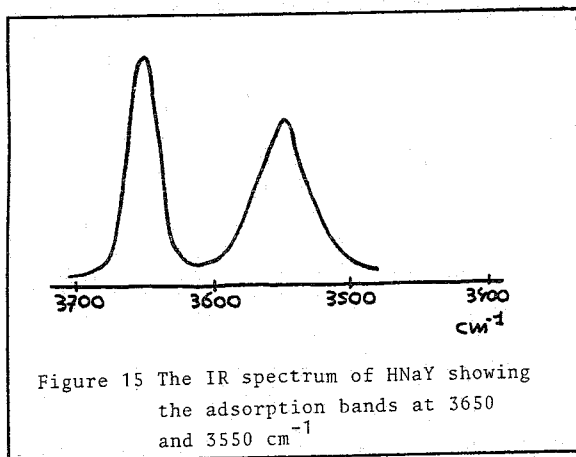figure 15).



Figure 15 The IR spectrum of HNaY showing
the adsorption bands at 3650
and 3550 $cm^{-1}$

These two bands are usually indicated as the

high frequency (HF) band at 3650 $cm^{-1}$    and the
low frequency (LF) band at 3550 $cm^{-1}$.

Both bands can be ascribed to  Si – O – Al groups.
If $NH_3$ is added to the system both bands disappear rapidly,
indicating the acid-properties of the OH groups.
However, if pyridine is used only the HF band disappears and the
LF-band stays almost unchanged. This can be explained by the
different positions of the OH groups in the zeolite structure;
the OH group causing the HF-band is situated in the supercages
and therefore easily accessible for a pyridine molecule. On the
contrary the position of the OH-group causing the LF-band is in
the hexagonal prism and thus inaccessible for pyridine (see
figure 16).

Figure 16 The two possible positions of
the OH groups in HNaY

easy accessible
HF band

inaccessible
LF band
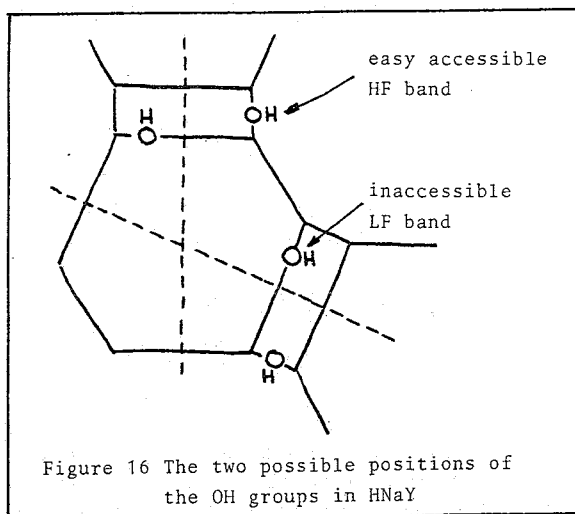
Lewis-acid groups cannot be detected directly by IR spectroscopy.
However, after the adsorption of pyridine it is possible.
On Brønsted-acid sites pyridine is adsorbed in the form of
pyridinium ions while on Lewis-acid sites the adsorption takes
place via a coordinative bond (see figure 17), leading to different
IR spectra (see figure 18).

Figure 17 The bonding of pyridine on a Brønsted- and
a Lewis-acid site
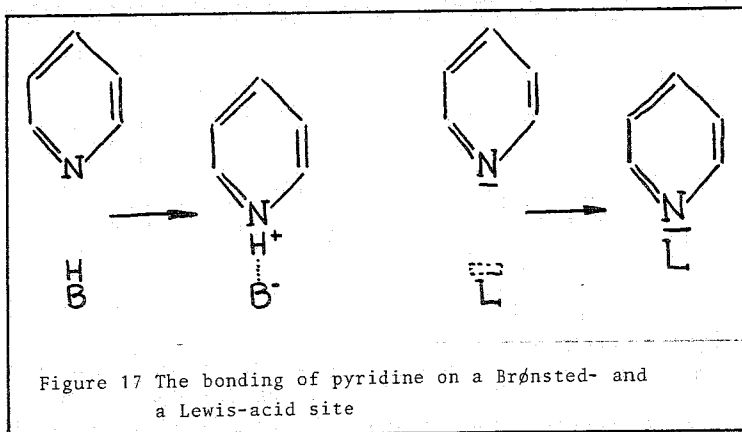
The pyridinium ion has absorption bands at 1540 and 1636 $cm^{-1}$ and
the coordinative bonded pyridine at 1450 and 1615 $cm^{-1}$

Figure 18 The IR spectrum of pyridine adsorbed on
Brønsted-(B) and Lewis-(L) acid sites
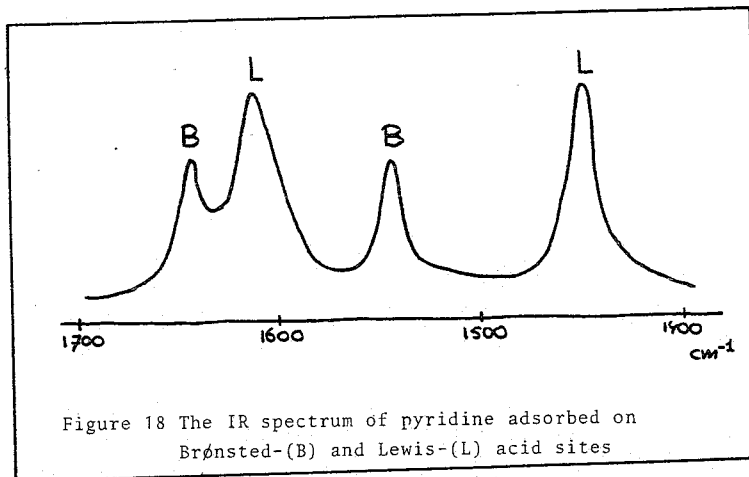
## APPLICATION OF RENaY AS CRACKING CATALYST

In the preceeding paragraphs it is shown that RENaY has
acid properties and therefore it may be used as a cracking
catalyst. However, two practical problems have to be solved first.

### i. The activity of pure RENaY is too high

For gasoil cracking the activity of pure RENaY is about 100 times
higher than of a low-alumina equilibrium catalyst. Therefore
application of pure RENaY in commercial cat-crackers, even after
modification is impossible.

### ii. The RENaY zeolite particles are too small

The average particle-size of the RENaY zeolite is about 1-10 μm.
This in combination with a particle density of 2.5 g/ml makes
application of pure RENaY in a fluid bed reactor impossible; the
small particles will be trailed by the gasstream and will pass
the cyclones.

To solve these problems the RENaY zeolite particles can be
embedded in a matrix. For example 5-25% RENaY can be embedded
in low-alumina and from this mixture particles can be formed that
can be used in a fluid bed reactor (average particle size about
60 μm). If we compare the performance of such a zeolite containing
catalyst with an amorphous low-alumina catalyst we obtain the
following picture.

|  | LA catalyst 100% LA | RENaY catalyst 10% RENaY 90% LA |
|---|---|---|
| relative activity for gasoil cracking | 100 | 1000 |
| selectivity at 75% conversion |  |  |
| gas | 15 | 10 |
| gasoline | 45 | 55 |
| light cycle oil | 10 | 7.5 |
| coke | 5 | 2.5 |

Compared with LA the zeolite catalyst has a much higher activity that allows much higher spacevelocities to obtain the same conversions. Furthermore the selectivity has drastically changed.

The selectivity for gasoline has been improved of the cost of the production of gas, light cycle oil and coke.

But also the composition of the gasoline has been changed [4]

| Gasoline composition | LA catalyst | Zeolite catalyst |
|---|---|---|
| Paraffins | 10 | 20 |
| Olefins | 45 | 15 |
| Naphthenes | 10 | 20 |
| Aromatics | 35 | 45 |

These differences can be explained by the relatively high rates of hydrogen transfer reactions in zeolites [10, 11].

Olefins, the primary cracking products, can be transformed to paraffins and aromatics according to the following reaction equation

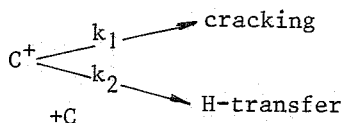$$4\ CnH_{2n} \longrightarrow 3\ CnH_{2n+2} + CnH_{2n-6}$$
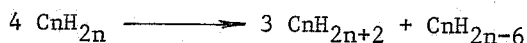
4 olefins          3 paraffins   aromatic

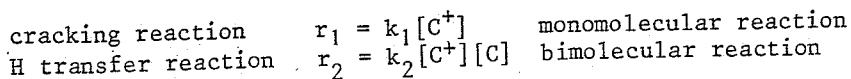The relatively high rate of this reaction in zeolites can be understood in the following way:

carbenium ions can undergo two distinct reactions

i.  they can be cracked by β-fission

ii. they can undergo a H-transfer reaction.

Schematically

*J.H.C. van Hooff*

The rates of these reactions are given by

cracking reaction $\quad r_1 = k_1[C^+] \quad$ monomolecular reaction
H transfer reaction $\quad r_2 = k_2[C^+][C] \quad$ bimolecular reaction

The ratio between these two rates can be expressed as

$$\frac{\text{rate H-transfer reaction}}{\text{rate cracking reaction}} = \frac{k_2[C^+][C]}{k_1[C^+]} \approx k'[C]$$

Thus the rate of the H-transfer reaction is favoured by a high hydrocarbon concentration [C] at the surface of the catalyst. This especially is the case in the small pores of the zeolites.

REFERENCES

1. C. Okkerse in B.C. Linsen (ea) 'Physical and Chemical Aspects of Adsorbents and Catalysts', p. 213 Academic, New York 1970.
2. Akzo Chemie, brochure of Ketjen catalysts.
3. C.J. Planck and E.J. Rosinski, Chem. Eng. Progr. 63, 26, 1967.
4. S.C. Eastwood, C.J. Planck and P.B. Weisz, Proc. 8th World Petr. Congr. Moscow, 1971.
5. D.W. Breck, 'Zeolite Molecular Sieves', Wiley, New York, 1974.
6. J.V. Smith, Adv. Chem. Ser. 101, 171, 1971.
7. H.A. Benesi, J. Am. Chem. Soc. 78, 5490, 1956, and J. Phys. Chem. 61, 970, 1957.
8. L. Moscou, R. Moné, J. Catalysis, 30, 417, 1973.
9. J.W. Ward in J.A. Rabo (ea) 'Zeolite Chemistry and Catalysis' Amer. Chem. Soc., Washington, 1976.
10. C.L. Thomas and D.S. Barmby, J. Catalysis 12, 341, 1968.
11. P.B. Weisz, Chemtech, August 1973, p. 498.